HIGH-PRESSURE PHYSICS

Synthesis of FeH_5: A layered structure with atomic hydrogen slabs

C. M. Pépin,[1,2]* G. Geneste,[1] A. Dewaele,[1] M. Mezouar,[3] P. Loubeyre[1]*

High pressure promotes the formation of polyhydrides with unusually high hydrogen-to-metal ratios. These polyhydrides have complex hydrogenic sublattices. We synthesized iron pentahydride (FeH_5) by a direct reaction between iron and H_2 above 130 gigapascals in a laser-heated diamond anvil cell. FeH_5 exhibits a structure built of atomic hydrogen only. It consists of intercalated layers of quasicubic FeH_3 units and four-plane slabs of thin atomic hydrogen. The distribution of the valence electron density indicates a bonding between hydrogen and iron atoms but none between hydrogen atoms, presenting a two-dimensional metallic character. The discovery of FeH_5 suggests a low-pressure path to make materials that approach bulk dense atomic hydrogen.

Dense metal hydrogen is expected to possess intriguing properties associated with the light mass and quantum behavior of the proton, such as a room-temperature superconductivity or even a superfluid/superconductor fluid state (*1*, *2*). We should observe atomic metal hydrogen around 450 GPa; however, achieving such a pressure with static compression is a major challenge. An alternate approach to high-temperature superconductivity of dense metal hydrogen is through hydrogen-rich alloys at much lower pressures (*3*). Many density functional theory calculations show, for numerous elements, pressure favoring the stability of polyhydrides with high stoichiometry. These polyhydrides might be superconductors with a critical temperature (T_c) approaching ambient temperature (*4*, *5*). The richness of this line of research has been confirmed by the discovery of superconductivity in hydrogen sulfide at a T_c of 203 K at 150 GPa, explained by the formation of H_3S (*6*, *7*). Furthermore, polyhydrides with unusually high H/M (H, hydrogen; M, metal) ratios were shown to exist with the observations of LiH_6 and NaH_7, which contain H_2 units (*8*, *9*). The progression in the discovery of these polyhydrides suggests a compound with a very high H content, which would be a real analog for atomic metal hydrogen.

The existence of alkali and alkaline earth polyhydrides is a topic investigated with a variety of methods and seemed the most promising route to reach very high H stoichiometries (*10*). However, the polyhydrides of these two groups of elements contain complex hydrogenic sublattices composed of H^-, H_2, H_3^-, or cage units. For other group elements, the richest stoichiometry is generally associated with the presence of quasi-molecular H_2 or H_3 units (*11*–*13*). On the other hand, trends disclosed by calculations on transition metal polyhydrides seem encouraging. Many H atoms can be bound to a metal atom forming molecules that are stabilized in matrices, potentially forming extended hydride structures. The hydrogen atoms should also remain in the H^- hydridic form even for the rich stoichiometry. With increasing hydrogen content, calculations predict that the dimensionality of the metal network decreases along with the emergence of layers of H atoms (*14*–*16*). The use of high hydrogen pressure has been very efficient in producing hydrides of transition metals, most being interstitial hydrides with an H/M ratio close to 1. Few larger H contents are obtained for the interstitial stoichiometric compounds RhH_2, IrH_3, FeH_2, and FeH_3 (*17*–*19*). In contrast, we synthesized a FeH_5 polyhydride with a prominent layered structure.

Epsilon iron hydride (ε′-FeH_x, $x \leq 1$) is an extensively studied archetypical interstitial hydride (*20*, *21*). The compression of Fe in excess hydrogen allows synthesis of FeH_2 and FeH_3 (*19*). The high-pressure sequence FeH, FeH_2, and FeH_3 was the clear experimental confirmation of the trend for hydrogen solubility to increase in metals determined theoretically by formation of unusual polyhydrides.

We compressed a 2-μm-thick Fe polycrystalline sample surrounded by excess hydrogen in a diamond anvil cell, similar to previous work (*19*). The diamond culets were 100 μm, and we performed

[1]Commissariat à l'Energie Atomique et aux Energies Alternatives, DAM, DIF, F-91297 Arpajon, France. [2]Earth and Planetary Science Laboratory, Institute of Condensed Matter Physics, Ecole Polytechnique Fédérale de Lausanne, CH-1015 Lausanne, Switzerland. [3]European Synchrotron Radiation Facility, 6 Rue Jules Horowitz BP220, F-38043 Grenoble CEDEX, France.
*Corresponding author. Email: charles.pepin@epfl.ch (C.M.P.); paul.loubeyre@cea.fr (P.L.)

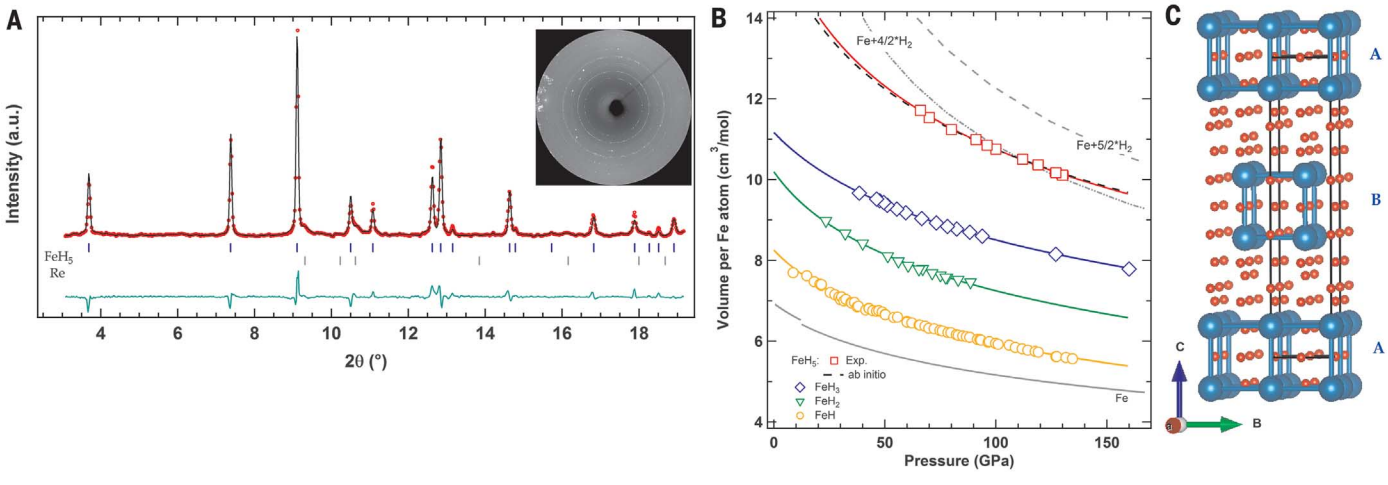

Fig. 1. Equation of state and structure determination of FeH_5. (**A**) Powder x-ray diffraction pattern and Rietveld refinement of the structure (iron atoms only) at 130 GPa for λ = 0.3738 Å. Vertical ticks correspond to the Bragg peaks for *I4/mmm*-FeH_5 and hexagonal close-packed–rhenium (gasket material). The conventional reliability factors for the Rietveld refinement are (in %) $RBragg_{(FeH5)}$ = 8.72, R_p = 19.3, R_{wp} = 17.3. (Inset) Image plate. (**B**) Molar volume per formula unit as a function of pressure for iron hydrides (*19*). The Vinet fits (*22*) of the data are full lines. Ab initio calculations are the black dashed line. Dash/dotted gray lines depict the molar volumes of ideal mixtures of iron and molecular hydrogen with H:Fe ratio of 4 and 5 using the previously determined equations of state (*33*, *34*). (**C**) Model representation of the FeH_5 structure. Large blue and small red spheres represent the iron and hydrogen atoms, respectively.

on-line yttrium-aluminum-garnet laser heating of the sample up to 150 GPa on the ID27 x-ray diffraction (XRD) beamline of the European Synchrotron Radiation Facility. The temperature was kept below 1500 K to avoid parasitic chemical reaction of hydrogen with the sample chamber wall and prevent diffusion of hydrogen in the diamond anvil. We collected angular XRD patterns before and about 1 min after laser heating. We confirmed the formation of simple cubic FeH_3 by laser heating of our samples between 100 and 125 GPa (*19*). New XRD peaks (Fig. 1A) appeared when the sample was laser-heated at 130 to 140 GPa. We found the same results on a second sample loading. The Rietveld refinement, using the FULLPROF software, of the diffraction pattern recorded at 130 GPa yields a tetragonal unit cell with the symmetry *I4/mmm* with $a = b = 2.404$ Å and $c = 11.621$ Å, with iron atoms in Wyckoff position *4e* (0, 0, 0.896) (Fig. 1A). The low scattering power of hydrogen atoms prevents the determination of their positions and consequently the stoichiometry using XRD. We measured the equation of state of this phase by decreasing pressure down to 66 GPa at ambient temperature (Fig. 1B). It decomposes back to FeH_3 below this pressure. The volume as a function of pressure [$V(P)$] data points can be fitted with a Vinet-type equation of state (*22*) with ambient pressure volume $V_0 = 16.447$ (±0.19) cm^3/mol, bulk modulus $K_0 = 85.9$ (±4.5) GPa, and its pressure derivative $K'_0 = 5$ (fixed).

We compared the compression curve of this FeH_x compound to the equations of state of FeH, FeH_2, FeH_3, and ideal Fe–H_2 solutions (Fig. 1B). We found a larger volume per Fe in our samples than in FeH_3, thus suggesting a substantial increase of the H/Fe ratio concentration. The $V(P)$ curve of the FeH_x compound lies above the ideal mixing line of Fe and 4/2 × H_2 solids and below the ideal mixing line of Fe and 5/2 × H_2. This indicates that a stoichiometry of 4 would make FeH_4 energetically less favorable with respect to the decomposition into the elements. The volume increase per H atom going from FeH to FeH_2 and from FeH_2 to FeH_3 is very similar—~1.9 $Å^3$ around 100 GPa (*19*)—and going from FeH_3 to FeH_x compound is twice this value. This suggests that FeH_5 may be an appropriate stoichiometry to explain our data.

We used the ABINIT code (*23*) and the projector-augmented wave method (*24*) for first-principles density functional calculations to determine the structural positional parameters of the hydrogen atoms in FeH_5 (*25*). We employed the generalized gradient approximation in the Perdew-Burke-Ernzerhof form (GGA-PBE) (*26*) that enabled us to satisfactorily calculate the properties of FeH, FeH_2, and FeH_3 (*19*). When we assumed the experimental determination of the Fe sublattice, we retained, among all structures compatible with the possible Wyckoff positions of a tetragonal *I4/mmm* unit cell (with Fe atoms in a *4e* position), 53 structures (*25*) and structurally optimized all of them. The minimum enthalpy at 147 GPa among these various structures is obtained with H atoms in Wyckoff positions *8g* (0, 0.5, 0.185), *4e* (0, 0, 0.4095), *4e* (0, 0, 0.230), and *4c* (0, 0.5, 0). This lowest enthalpy structure for FeH_5 (Fig. 1C and fig. S1) is a structure formed by alternating layers of FeH_3 and hydrogen atoms. Phonons calculation shows that this structure is dynamically stable (*25*). Furthermore, two molecular dynamic runs in the isobaric-isothermal (N, P, T) ensemble confirm the stability: This structure is unchanged after a molecular dynamic run and is obtained after starting from a higher energy structure (*25*). Finally, the compression curve calculated for this FeH_5 structure is in excellent agreement with our experimental data (Fig. 1B). We found good agreement comparing the experimentally and computationally determined lattice parameters (fig. S2). The c axis is more compressible than the a axis, which is in line with our preferred structure (Fig. 1C), where the strongest bonds are expected to lie in the (ab) plane. The FeH_5 structure has the same space group *I4/mmm* as FeH_2, with Wyckoff positions for the Fe atoms that are almost identical [*4e* (0, 0, 0.853) for FeH_2 and *4e* (0, 0, 0.896) for FeH_5]. FeH_5 also has structural similarities to a simple cubic FeH_3. The layers containing Fe and H atoms are composed of quasisimple cubic FeH_3 units, similar to the FeH_3 structure, sharing faces (the Fe–Fe distances are 2.404 Å along the x and y axis and 2.414 Å along the z axis) arranged in an ABAB stacking. These FeH_3 units are slightly bigger than in pure FeH_3, which has a cell parameter of 2.38 Å at 130 GPa.

The structures of the Fe polyhydrides stable in excess hydrogen have increasing stoichiometry with increasing pressure and, as previously suggested (*14*–*16*), decreasing dimensionality of the associated metal network due to the intercalation of the H layers (Fig. 2). Experimentally, we did not observe the predicted $P2_1/m$-, $P2_13$-, and *Imma*-structured FeH_4 (*27*, *28*). Our calculations also allow us to propose a *Cmmm*-structured FeH_4 not previously considered (*27*, *28*) (fig. S5). However, the Hull plot (fig. S3) shows that FeH_4 is never stable against decomposition. FeH_5 is stable against decomposition between FeH_3 and H_2 above 55 GPa. Therefore, the high stability of FeH_5 above 55 GPa hinders the formation of FeH_4.

We compared the H–H nearest-neighbor distance in the dense atomic hydrogen slab of FeH_5 to the nearest-neighbor H distance for polyhydrides in which neither quasimolecular H_2 nor H_3 units are formed (Fig. 2B). At 130 GPa the nearest H–H distance is 1.32 Å, which is considerably lower than the ~1.70 Å value in FeH_3. Aluminum hydride (AlH_3) has a nonbonded H–H distance 1.53 Å at 130 GPa (*29*). A similar value of ~1.5 Å was found in the high-temperature superconducting phase of H_3S (*5*, *30*). The shortest H–H distance in FeH_5 is thus the closest to the shortest H–H distance in atomic metal hydrogen, artificially extended in the same pressure range (Fig. 2C) (*25*). The volume expansion due to the addition of one hydrogen in the FeH_x formula unit is constant at a given pressure and is close to the volume of atomic metal hydrogen (Fig. 2C).

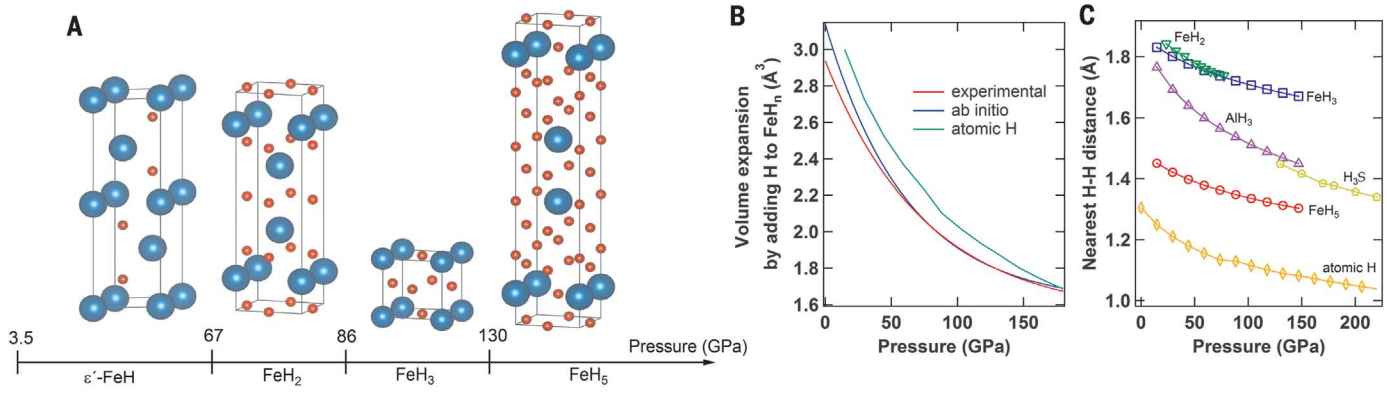

Fig. 2. Hydrogen in the host lattice. (**A**) Evolution of the stoichiometry and of the structures of iron hydrides synthesized in excess of hydrogen as the pressure increases. (**B**) Volume expansion by adding one H to FeH_n, compared to the equation of state of pure atomic hydrogen. The volume expansion is determined as the slope of the equation V(FeH_n) versus stoichiometry at various pressures. (**C**) Comparison of the nearest H–H distances in AlH_3 (*29*), H_3S (*30*), FeH_2, FeH_3 (*19*), metal H (*25*), and FeH_5 as a function of pressure.

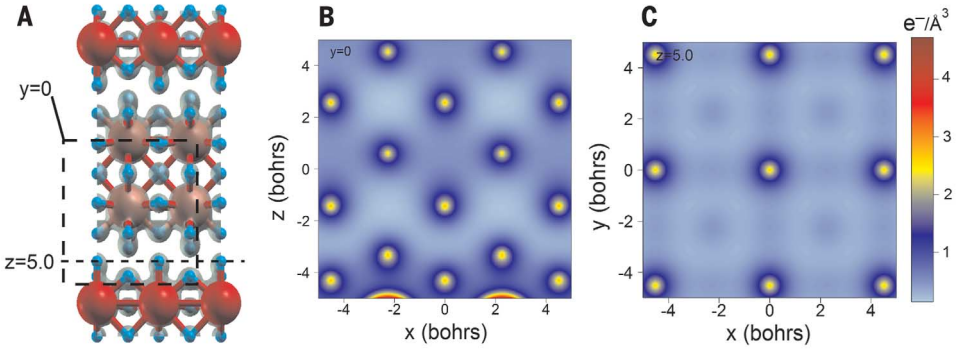

Fig. 3. Electron-density distribution at 147 GPa. (**A**) Structure of FeH_5 showing the isosurface for the electron density of 0.8 el/Å^3. (**B**) Electron density map in the plane y = 0 as shown on the truncated structure. The large hidden spheres at the bottom around x = −2 and 2 bohrs are iron atoms. (**C**) Electronic density map in a plane perpendicular to the c axis as shown on the truncated structure. The hydrogen atom in position (0, 0, 0.23) is taken as the reference position (0, 0).

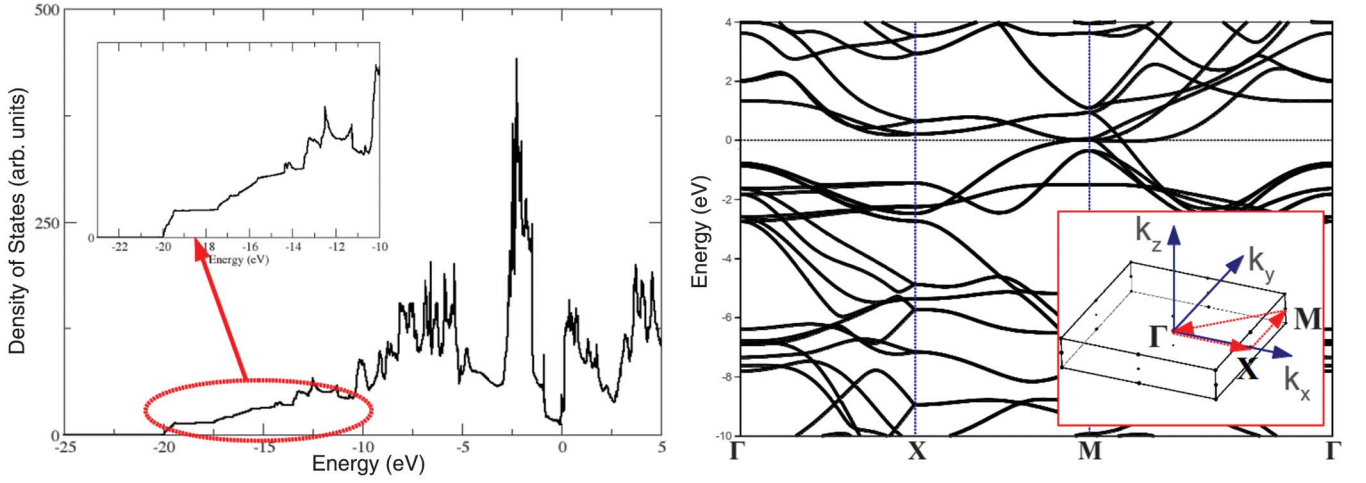

Fig. 4. Band structure and electronic densities of state of FeH_5 at 147 GPa. (Left) Electronic density of states of FeH_5. (Right) Electronic band structure plotted on a path in the k_z = 0 plane. (Inset) View of the Brillouin zone of the conventional unit cell, with the path used to plot the band structure (red arrows). The Fermi level is set at 0 eV in both cases.

Hence, the formation of Fe polyhydrides can be viewed as an ideal mixing of Fe and atomic metal H and associated, for a large fraction of metal H (*25*), with the formation of a thicker atomic H slab in the structure of the polyhydride.

The electron-density distribution (Fig. 3) gives a qualitative indication of the bonding in FeH_5. The valence electron density is nonuniform in space (Fig. 3A). The higher electron density between Fe and H suggests bonding between them. Thirteen H atoms bond to each Fe atom, 12 of them bridging two Fe atoms, and the remaining one has a single Fe–H bond parallel to c ("top" H). The ABAB stacking of FeH_3 units allows a compact arrangement of "top" H atoms. Many hydrogen atoms can be bound to a transition metal atom (*31*), although only FeH, FeH_2, and FeH_3 molecules could be isolated in matrices at ambient pressure (*32*). We visualized the electron density distribution in the plane parallel to the stacking direction, also showing the H–Fe bonding (Fig. 3B). The electron density in the plane of the hydrogen atoms is more uniform (Fig. 3C), with a minimum value 3.6 times lower (0.3 el/Å^3) than that along Fe–H. It clearly shows that no H–H bonding exists. The topology of the electron density seems to give a different representation of the FeH_5 structure than the geometrical one, more as a stacking of alternate FeH_5 layers reminiscent of two-dimensional (2D) van der Waals materials. The reality is probably in between, with the atomic H slab interacting with the Fe atoms to stabilize dense atomic H at a much lower pressure than in pure hydrogen, in the spirit of the chemical "precompression" proposed by Ashcroft (*3*).

We also calculated the band structure and the electronic densities of states (DOS) for FeH_5 (Fig. 4). The DOS has a clear steplike character at the bottom of the occupied band, indicating that electronically FeH_5 is also a 2D metal. In this range, the DOS is constituted by H 1*s* and Fe 4*s* orbitals. Yet, there is a clear depletion of the DOS near the Fermi level, so FeH_5 should be considered as a weak metal. The electronic band structure, as drawn in Fig. 4B, shows that the bandgap closure is only effective for a few points at the Brillouin-zone corners.

The series of Fe polyhydrides, from FeH to FeH_5, present an example of how hydrogen can combine with transition metals as pressure increases. Remarkably, the structures of these polyhydrides are built of atomic hydrogen only. By increasing pressure, hence the H content, slabs of atomic hydrogen are stabilized, giving, as in an FeH_5 structure, structures resembling bulk atomic hydrogen. The next step would now be to quantify in FeH_5 some of the intriguing quantum effects of atomic hydrogen.

REFERENCES AND NOTES

1. N. W. Ashcroft, *Phys. Rev. Lett.* **21**, 1748–1749 (1968).
2. E. Babaev, A. Sudbø, N. W. Ashcroft, *Nature* **431**, 666–668 (2004).
3. N. W. Ashcroft, *Phys. Rev. Lett.* **92**, 187002 (2004).
4. E. Zurek, R. Hoffmann, N. W. Ashcroft, A. R. Oganov, A. O. Lyakhov, *Proc. Natl. Acad. Sci. U.S.A.* **106**, 17640–17643 (2009).
5. H. Wang, J. S. Tse, K. Tanaka, T. Iitaka, Y. Ma, *Proc. Natl. Acad. Sci. U.S.A.* **109**, 6463–6466 (2012).
6. A. P. Drozdov, M. I. Eremets, I. A. Troyan, V. Ksenofontov, S. I. Shylin, *Nature* **525**, 73–76 (2015).
7. I. Troyan *et al.*, *Science* **351**, 1303–1306 (2016).
8. C. Pépin, P. Loubeyre, F. Occelli, P. Dumas, *Proc. Natl. Acad. Sci. U.S.A.* **112**, 7673–7676 (2015).
9. V. V. Struzhkin *et al.*, *Nat. Commun.* **7**, 12267 (2016).
10. E. Zurek, *Comments Inorg. Chem.* **37**, 78–98 (2017).
11. X. Zhong *et al.*, *Phys. Rev. Lett.* **116**, 057002 (2016).
12. P. Zaleski-Ejgierd, R. Hoffmann, N. W. Ashcroft, *Phys. Rev. Lett.* **107**, 037002 (2011).
13. M. Somayazulu *et al.*, *Nat. Chem.* **2**, 50–53 (2010).
14. P. Zaleski-Ejgierd, V. Labet, T. A. Strobel, R. Hoffmann, N. W. Ashcroft, *J. Phys. Condens. Matter* **24**, 155701 (2012).
15. X. Feng *et al.*, *Solid State Commun.* **239**, 14–19 (2016).
16. S. Yu *et al.*, *Sci. Rep.* **5**, 17764 (2015).
17. B. Li *et al.*, *Proc. Natl. Acad. Sci. U.S.A.* **108**, 18618–18621 (2011).
18. T. Scheler *et al.*, *Phys. Rev. Lett.* **111**, 215503 (2013).

19. C. M. Pépin, A. Dewaele, G. Geneste, P. Loubeyre, M. Mezouar, *Phys. Rev. Lett.* **113**, 265504 (2014).
20. J. V. Badding, R. J. Hemley, H. K. Mao, *Science* **253**, 421–424 (1991).
21. N. Hirao, T. Kondo, E. Ohtani, K. Takemura, T. Kikegawa, *Geophys. Res. Lett.* **31**, L06616 (2004).
22. P. Vinet, J. R. Smith, J. Ferrante, J. H. Rose, *J. Phys. Chem.* **19**, L46 (1987).
23. X. Gonze *et al.*, *Z. Kristallogr.* **220**, 558 (2005).
24. M. Torrent, F. Jollet, F. Bottin, G. Zerah, X. Gonze, *Comput. Mater. Sci.* **42**, 337–351 (2008).
25. Materials and methods are available online as supplementary materials.
26. J. P. Perdew, K. Burke, M. Ernzerhof, *Phys. Rev. Lett.* **77**, 3865–3868 (1996).
27. Z. Bazhanova, A. Oganov, O. Gianola, *Phys. Uspekhi* **55**, 489–497 (2012).
28. F. Li *et al.*, *RSC Advances* **7**, 12570–12575 (2017).
29. I. Goncharenko *et al.*, *Phys. Rev. Lett.* **100**, 045504 (2008).
30. D. Duan *et al.*, *Sci. Rep.* **4**, 6968 (2014).
31. L. Gagliardi, P. Pyykkö, *J. Am. Chem. Soc.* **126**, 15014–15015 (2004).
32. G. V. Chertihin, L. Andrews, *J. Phys. Chem.* **99**, 12131–12134 (1995).
33. A. Dewaele *et al.*, *Phys. Rev. Lett.* **97**, 215504 (2006).
34. P. Loubeyre *et al.*, *Nature* **383**, 702–704 (1996).

ACKNOWLEDGMENTS

The authors acknowledge the European Synchrotron Radiation Facility for provision of synchrotron radiation on beamline ID27 (proposal HC-1914). Data are available on request. The authors declare no conflict of interest.

SUPPLEMENTARY MATERIALS

www.sciencemag.org/content/357/6349/382/suppl/DC1
Materials and Methods
Supplementary Text
Figs. S1 to S6
Tables S1 to S3
Data S1
References (*35*–*40*)

3 March 2017; accepted 22 June 2017
10.1126/science.aan0961

Science

Synthesis of FeH_5: A layered structure with atomic hydrogen slabs

C. M. Pépin, G. Geneste, A. Dewaele, M. Mezouar and P. Loubeyre

Science **357** (6349), 382-385.
DOI: 10.1126/science.aan0961

Atomic hydrogen with an iron assist

Metal polyhydrides can be used at lower pressures to make material that might have atomic hydrogen bonding. Pépin *et al.* manage to synthesize an incredibly hydrogen-rich FeH_5 compound at 130 GPa pressure. The material consists of slabs of four thin planes of atomic hydrogen intercalated with layers of quasicubic FeH_3 units. These metal polyhydrides were stable at far more accessible pressures than pure hydrogen. This achievement provides an opportunity to investigate special electrical properties expected from atomic hydrogen bonding, such as superconductivity.

Science, this issue p. 382